Available online at www.sciencedirect.com
ScienceDirect
Scripta Materialia 64 (2011) 398–401
Scripta MATERIALIA
www.elsevier.com/locate/scriptamat

Atomistic simulations of dislocation–precipitate interactions emphasize importance of cross-slip

C.V. Singh,[a] A.J. Mateos[b] and D.H. Warner[a,*]

[a] *School of Civil and Environmental Engineering, Cornell University, Ithaca, NY 14853, USA*
[b] *Department of Mechanical Engineering, Texas A&M University, College Station, TX 77843, USA*

Received 15 October 2010; revised 27 October 2010; accepted 28 October 2010
Available online 2 November 2010

This work examines the interaction of screw dislocations with Guinier–Preston (GP) zones using atomistic simulations. Both Orowan looping and cross-slip mechanisms are found to control the interactions. Cross-slip, occurring both at zero and finite temperatures, is found to either significantly reduce or enhance precipitate strengthening, depending upon the orientation of the dislocation–GP zone interaction. The orientation dependence, and its dependence on temperature, provides a micromechanical explanation for the experiments of Muraishi et al. (Philos. Mag. A 82 (2002) 2755).

Keywords: Aluminium alloys; Molecular dynamics; Precipitation hardening; Dislocation–obstacle interaction; Cross-slip

The strength of many engineering alloys can be attributed to the presence of submicron precipitates, which inhibit the motion of dislocations. Perhaps one of the most popular and long-standing examples involves Al–Cu alloys, where flow strength can be enhanced by more than a factor of three using a heat treatment schedule to generate a dense array of precipitates in the material [1]. Over the past century, treatments have advanced to the point where precipitation-hardened Al alloys with near-gigapascal strengths are now possible [2,3]. For further improvements of alloy performance into the next century, a knowledge of the controlling micromechanics of dislocation–precipitate interactions will need to be exploited.

Efforts to illuminate dislocation–precipitate interactions span more than 60 years [4–10]. With regard to mechanisms, it is widely agreed that dislocations overcome shearable precipitates via cutting, and impenetrable precipitates via Orowan looping. Additionally, dislocations are hypothesized to overcome precipitates via formation of prismatic loops involving cross-slip and climb [11,12]. Within the last decade, atomistic simulations have also begun to contribute to our understanding of dislocation–precipitate interactions [13–15,17,16,18,19]. As a whole, these simulations have confirmed many classical ideas, while they also have unveiled a vast complexity of dislocation precipitate interactions. The present work, focused on screw dislocation–precipitate interactions, is consistent with this theme.

After introducing the methodology, this letter reports on observations of screw dislocations overcoming precipitates via cross-slip. The cross-slip mechanism has a significant impact on macroscopic response as the stress required to move a dislocation past a precipitate can decrease by more than a factor of six compared to cases where cross-slip does not occur. The second finding reported in this manuscript is the observation of a cross-slip strengthening mechanism, where the cross-slip of a dislocation near a precipitate does not provide a clear route of glide away from the precipitate and ultimately requires a significantly higher applied stress for the dislocation to overcome the precipitate. In both the traditional and hardening cases of cross-slip, the mechanisms are observed to occur in both the absence and presence of thermal activation, with cross-slip hardening being significantly temperature dependent. As a whole, these findings, when considered alongside of edge dislocation–precipitate interactions studied in our previous work [19], provide an explanation for the orientation dependence of strengthening effects observed in the experiments by Eto et al. [20] and Muraishi et al. [21].

The specific precipitate chosen for this study is a Guinier–Preston (GP) zone [22,23]. GP zones are nanometer-sized monolayered disks that form during the early stages of age hardening and are common to many alloys, e.g. Al–Cu, Al–Zn, Al–Cu–Zn, Cu–Be, Fe–Mo, Al–Ag

* Corresponding author. Tel.: +1 607 255 7155; fax: +1 607 255 9004; e-mail: dhw52@cornell.edu

1359-6462/$ - see front matter © 2010 Acta Materialia Inc. Published by Elsevier Ltd. All rights reserved.
doi:10.1016/j.scriptamat.2010.10.041

and Al–Mg–Si. The technologically relevant Al–Cu material system is the focus of this work. We consider the composition of GP zones to be 100% Cu, although experimental reports do vary [24,25].

Considering dislocations of pure screw or edge character limits the possible dislocation–GP zone interactions to four orientations since GP zones only form on {1 0 0}-type planes. We classify these orientations by the dislocation character, i.e. screw or edge, and the angle between the dislocations' Burgers vector and the plane of the GP zone, i.e. 0° or 60° (Fig. 1).

The atomistic simulations were carried out using the freely available open source LAMMPS code [26]. The code was modified to use a recently developed Al–Cu empirical potential developed by Apostle and Mishin [27]. The potential is an angular dependent extension of the popular embedded atom method [28,29].

The simulation cell (Fig. 1) consisted of an Al face-centered cubic lattice, bounded by $(1\,1\,\bar{2})$, $(1\,1\,1)$, and $(\bar{1}\,1\,0)$ faces in the X, Y and Z directions, respectively. Periodic boundary conditions were applied in the X and Z directions, whereas the Y surfaces were used to apply the load. Starting from a perfect lattice, a GP zone was created by simply changing selected atom types to Cu. The continuum displacement field of a screw dislocation was used to create a dislocation in the center of the simulation cell ($X = Y = 0$) with a line direction parallel to the Z-axis and a Burgers vector of $\vec{b} = 1/2[\bar{1}\,1\,0]$. The simulation cell size was approximately $34 \times 42 \times 16$ nm^3 and contained approximately 1.4 million atoms. Based on our experience with edge dislocation–GP zone interactions [19], this size is sufficient to produce size-independent results in all directions except the dislocation line direction, where the critical stress at which a dislocation overcomes a GP zone varies inversely with GP zone spacing (cell size in Z-direction), $\tau_c \propto 1/L$, consistent with standard continuum analysis [4].

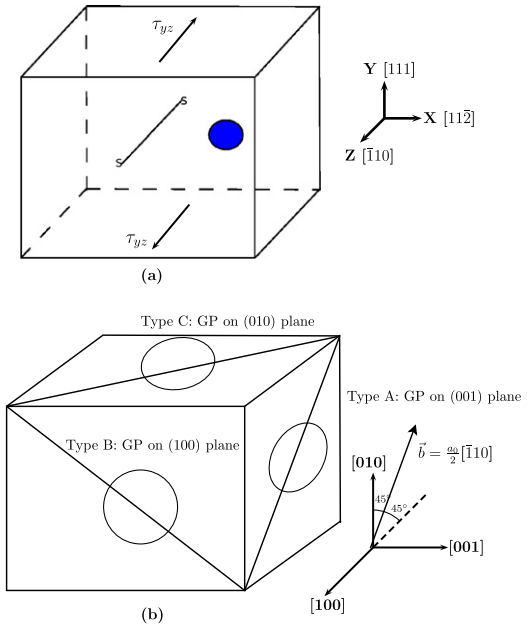

Figure 1. (a) Simulation cell with screw dislocation and GP zone. (b) Three possible GP zone orientations with respect to Burgers vector. Types B and C are equivalent.

Prior to loading, NPT dynamics at $T = 1$ K were performed for 30 ps to relax the system and alleviate out-of-balance forces and net stresses. The system was then loaded in shear by subjecting the atoms near the top and bottom Y surfaces to a constant traction. For the screw dislocation, the traction is τ_{yz}. The applied traction was increased at a constant quasi-static rate until the dislocation broke free from the GP zone. At each load step, nonlinear conjugate gradient minimization was performed until the out-of-balance forces became less than 10^{-8} eV/Å for the 0 K simulations. Molecular dynamics simulations were performed using a standard NVT approach.

We begin by examining the 60° screw dislocation–GP zone interaction. Upon the initial NPT relaxation from the continuum screw dislocation displacement field, the dislocation core dissociates into two partial dislocations spaced 0.6 nm apart. During relaxation, the center of the core remains stationary at 6.8 nm from the GP zone, suggesting that the elastic forces acting on the dislocation at this distance are below the Peierls stress (30 MPa). Figure 2a details the series of events that occur as applied loading is increased at 0 K for a 4.4 nm diameter GP zone that is intersected through its center by the (1 1 1) plane on which the dislocation resides. As the load is increased the dislocation begins moving towards the GP zone as the force from the applied load overtakes the Peierls stress and repulsion from GP zone. At $\tau_{yz} = 36$ MPa $(0.063\tau_{\text{Orowan}})$, where $\tau_{\text{Orowan}} = \frac{Gb}{L} = \frac{31.6\ \text{GPa} * 2.86\ \text{Å}}{158.7\ \text{Å}} \approx 570$ MPa is the theoretical Orowan stress [4]), the leading partial dislocation contacts the GP zone. At $\tau_{yz} = 42$ MPa $(0.074\tau_{\text{Orowan}})$ the dislocation cross-slips onto the $(1\,1\,\bar{1})$ plane, where it remains pinned until 45 MPa $(0.079\tau_{\text{Orowan}})$, at which point it glides away.

To investigate whether the above observation of cross-slip is representative of general behavior, multiple GP zone sizes and realizations were examined. In one of the cases, involving a 4.4 nm diameter GP zone, the dislocation did not cross-slip, but rather overcame the GP zone by Orowan looping [4] at a much higher applied load, $\tau_{yz} = 280$ MPa $(0.491\tau_{\text{Orowan}})$. This occurrence demonstrates three things. First, it shows that cross-slip in our geometry at 0 K is sensitive to variations in the exact atomic arrangement around the perimeter of the GP zone (noting that at finite temperature all cases exhibited cross-slip). Second, the critical stress required for a dislocation to overcome a GP zone in this orientation is much lower via cross-slip than via Orowan looping. Therefore, for this case, cross-slip acts as a relaxation mechanism. Third, it shows that Orowan looping can be favorable to cutting even for nanometer-sized precipitates.[1] This point is in contrast to conventional wisdom; however, we note that at experimental times and temperatures thermal activation may promote cutting. No significant correlation between GP zone size and applied stress for cross-slip was observed for the 60° interaction.

[1] We identify the Orowan looping mechanism by examining the Cu atoms of the GP zone after the dislocation has overcome the precipitate. Since these atoms do not show a displacement jump of a Burgers vector after being overcome by the dislocation, one can assume that a dislocation loop is created around the GP zone. See Ref. [19] for more details.

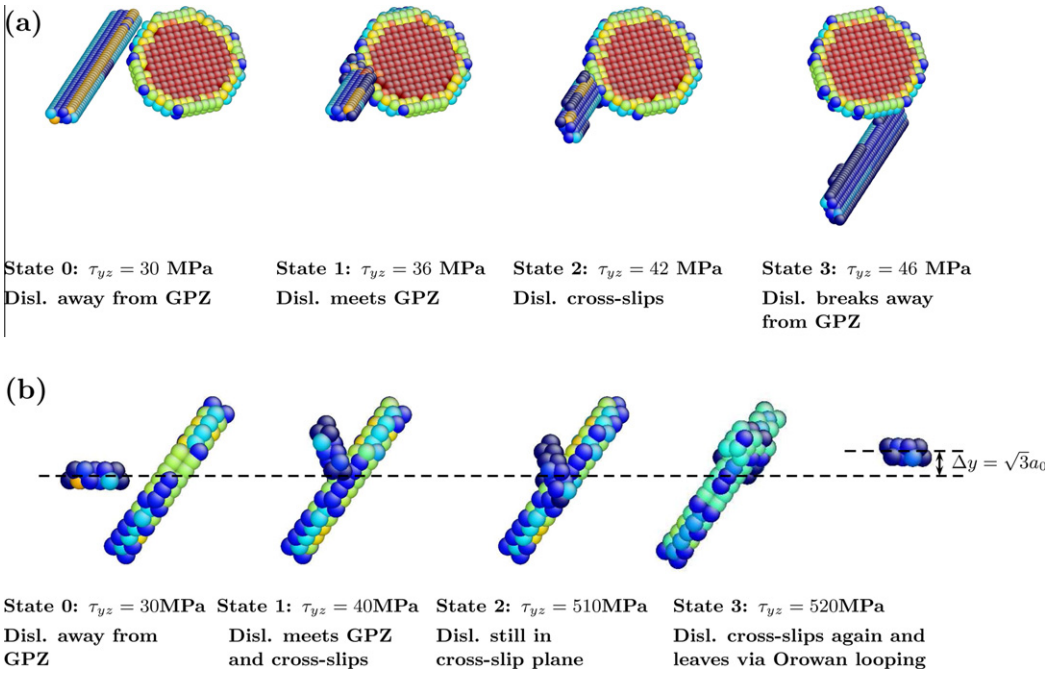

Figure 2. Dominant screw dislocation–GP zone interaction mechanisms at $T = 0$ K. (a) A 60° interaction where the dislocation cross-slips onto a glide plane unimpeded by the GP zone and easily glides away. (b) A 0° interaction where the dislocation cross-slips onto a glide plane impeded by the GP zone and requires a large applied stress to cross-slip back to a plane parallel to its original glide plane and ultimately overcome the GP zone via Orowan looping. The snapshots are shown by AtomEye visualization software [30] using "centro-symmetry parameter" [31] to plot only the defective atoms in the crystal.

The vertical offset between the center of the GP zone and the initial dislocation slip plane did have an effect on the mechanism and the applied shear stress at which the dislocation ultimately overcame the GP zone, τ_c. When the approaching dislocation slip plane was above the center point of the 4.4 nm GP zone (relative to Fig. 2a) the dislocation did not cross-slip, but rather it Orowan looped around the GP zone, with τ_c ranging between 270 and 310 MPa. When the intersection point was below the center point, cross-slip was always observed, with τ_c near 50 MPa.

Cross-slip also occurred for the 0° screw dislocation–GP zone interaction. Figure 2b details the series of events that occur as the applied loading is increased at 0 K for a 4.4 nm diameter GP zone centered on the dislocation glide plane. At $\tau_{yz} < 30$ MPa $(0.053\tau_{\text{Orowan}})$, the equilibrium position of the leading partial is 7 nm from the GP zone and no noticeable contraction of the core is evident. Between $\tau_{yz} = 30$ and 40 MPa the dislocation cross-slips from the $(1\,1\,1)$ to the $(1\,1\,\bar{1})$ plane, with the leading partial remaining stationary at the surface of the GP zone. Although the dislocation cross-slips to the $(1\,1\,\bar{1})$ plane, its forward motion is still obstructed by the GP zone. Furthermore, the applied force acting on the dislocation is now reduced by a factor of $\sqrt{3/2}$. The dislocation remains in this state until $\tau_{yz} = 520$ MPa $(0.912\tau_{\text{Orowan}})$, at which point it cross-slips back onto a $(1\,1\,1)$ plane and overcomes the GP zone via Orowan looping [4]. The $(1\,1\,1)$ plane that the dislocation ultimately resides on is $\Delta y = \sqrt{3}a_0$ above the original $(1\,1\,1)$ plane on which it started. Screw dislocation cross-slip in this case, in contrast to the 60° interaction, acts as a hardening mechanism. In a random field of obstacles where multiple mechanisms can occur along the dislocation line, only segments of the dislocation may cross-slip consistently with the early stages of the Hirsch mechanism for screw dislocations [11,12].

For the 0° interaction orientation, GP zone size was found to have an appreciable effect. For small sizes with diameters <3 nm, the dislocation cross-slipped at a position far enough away from the GP zone that it was then able to overcome the GP zone on the cross-slip plane. For larger sizes, however, the dislocation–GP zone interaction entailed the double cross-slip mechanism detailed above. For the 4.4 nm GP zone the offset between the center of the GP zone and the initial dislocation slip plane was studied and found to not have an effect on the underlying mechanism, though it did produce significant variations in τ_c, i.e. 400–700 MPa.

It is worth noting that for both interaction orientations cross-slip occurred during 0 K simulation in the absence of thermal activation. The same mechanisms were observed during the 300 K molecular dynamics simulations. For the 60° interaction no significant effect of thermal activation was observed with regard to τ_c (Table 1) at the loading rate examined, 5×10^{11} MPa s^{-1}. However, for the 0° interaction, τ_c demonstrated a significant temperature dependence, associated with the second cross-slip event. It is plausible that at 300 K and experimental rates/times the critical stress for the second cross-slip event back to the $(1\,1\,1)$ plane may decrease to a point where it is no longer the controlling mechanism that determines τ_c.

The influence of orientation on dislocation–GP zone interactions has been investigated experimentally by Eto et al. [20] and Muraishi et al. [21]. Their experiments

Table 1. Orientation and temperature dependence of τ_c for a GP zone with 4.4 nm diameter intersecting the slip plane through its center.

Dislocation character	GP zone orientation (°)	τ_c (MPa)	
		$T = 0$ K	$T = 300$ K
Screw	0	514	426
	60	45	45
Edge	0	185	169
	60	232	210

utilized Al–Cu specimens with GP zones aligned in a common direction. This allowed for the effect of the angle between the Burgers vectors of active dislocations and the GP zone planes to be examined collectively. The experiments revealed that at room temperature there is no noticeable effect of the Burgers vector–GP zone orientation on strength. However, at 77 K the strength of specimens with active dislocations having Burgers vectors parallel to the plane of GP zones showed a significantly enhanced strength. To connect the results of the simulations performed here with the experiments of Eto et al. and Muraishi et al., we utilize data from our previous work on edge dislocation–GP zone interactions [19] (Table 1). While the effective resistance to dislocation glide in experiment is likely to be a complex function of τ_c for both screw and edge dislocation characters, reasonable bounds can be assumed. A lower bound of effective glide resistance would consist of the arithmetic mean of τ_c from both screw and edge character dislocation–GP zone interactions. An upper bound would consist of only τ_c from the stronger dislocation character interaction. Regardless of which bound is considered, the atomistic simulation results are consistent with experiments in two important ways: (i) GP zones act as stronger obstacles to dislocation glide at 0 K when the Burgers vectors of active dislocations are parallel to the planes of GP zones due to the large strength increase associated with screw dislocations cross-slipping onto impeded planes. It should be noted that if only edge dislocations are considered the opposite conclusion contrasting experiment is reached and (ii) the strengthening effect from screw dislocations, with Burgers vectors parallel to GP zone planes, cross-slipping onto impeded planes varies inversely with temperature due to thermal activation aiding the second cross-slip event, while the other orientations and mechanisms show a much milder temperature dependence at molecular dynamics strain rates.

In summary, the atomistic simulations performed here have highlighted the importance of dislocation cross-slip in precipitation hardening. It is found that cross-slip can either decrease or increase the hardening effect of precipitates, depending upon whether the cross-slip plane is impeded by the precipitate. Cross-slip is observed to occur at both 0 and 300 K, suggesting that it can occur in the absence of thermal activation. The importance of cross-slip in precipitation hardening is highlighted when considering the simulation results in the context of experimental data which cannot be explained solely by edge dislocation precipitate interactions. When cross-slip does not occur or does not provide an unimpeded plane for the dislocation to overcome the precipitate, Orowan looping is observed in 0 K simulations. Considering that the precipitates are GP zones, this is in contrast to the long-held continuum view that dislocations overcome small precipitates via cutting. This analysis, in combination with our previous report [19], forms the foundation for atomistic-based modeling of age hardening, the focus of our forthcoming work.

The authors gratefully acknowledge support from Ed Glaessgen and Steve Smith at NASA (Grant No. NNX08BA39A). Support in part by the Cornell Center for Materials Research and the National Science Foundation is also acknowledged.

[1] J.M. Silcock, T.J. Heal, H.K. Hardy, J. Inst. Metals 82 (1953–1954) 239.
[2] P.V. Liddicoat, X.Z. Liao, Y. Zhao, Y. Zhu, M.Y. Murashkin, E.J. Lavernia, R.Z. Valiev, S.P. Ringer, Nat. Commun. 1 (2010) 1.
[3] R.Z. Valiev, N.A. Enikeev, M.Y. Murashkin, V.U. Kazykhanov, X. Sauvage, Scripta Mater. 63 (2010) 949.
[4] E. Orowan, Symposium on Internal Stresses in Metals and Alloys, Institute of Metals, London, 1948.
[5] N.F. Mott, F.R.N. Nabarro, Report of a Conference on Strength of Solids, The Physical Society, London, 1948, p. 1.
[6] A. Kelly, R.B. Nicholson, Prog. Mater. Sci. 10 (1963) 151.
[7] S.D. Harkness, J.J. Hren, Metall. Trans. 1 (1970) 43.
[8] D.J. Bacon, U.F. Kocks, R.O. Scattergood, Philos. Mag. 28 (1973) 1241.
[9] A. Ardell, Metall. Trans. 16 (1985) 2131.
[10] A. Argon, Strengthening Mechanisms in Crystal Plasticity, Oxford University Press, New York, 2007.
[11] P.B. Hirsch, J. Inst. Metals 86 (1957) 13.
[12] F.J. Humphreys, P.B. Hirsch, Proc. Royal Soc. Lond. A 318 (1970) 73.
[13] Y.N. Osetsky, D.J. Bacon, J. Nucl. Mater. 323 (2003) 268.
[14] T. Hatano, Phys. Rev. B 74 (2006) 020102.
[15] J.H. Shim, Y.W. Cho, S.C. Kwon, W.W. Kim, B.D. Wirth, Appl. Phys. Lett. 90 (2007) 021906.
[16] T. Hatano, T. Kaneko, Y. Abe, H. Matsui, Phys. Rev. B 77 (2008) 064108.
[17] D. Terentyev, G. Bonny, L. Malerba, Acta Mater. 56 (2008) 3229.
[18] Z. Chen, N. Kioussis, N. Ghoniem, Phys. Rev. B 80 (2009) 184104.
[19] C.V. Singh, D.H. Warner, Acta Mater. 58 (2010) 5797.
[20] T. Eto, A. Sato, T. Mori, Acta Metall. 26 (1978) 499.
[21] S. Muraishi, N. Niwa, A. Maekawa, S. Kumai, A. Sato, Philos. Mag. A 82 (2002) 2755.
[22] A. Guinier, Ann. Phys. 12 (1939) 161.
[23] G.D. Preston, Philos. Mag. 26 (1938) 855.
[24] K. Hono, T. Satoh, K.I. Hirano, Philos. Mag. A 53 (1986) 495.
[25] M. Karlik, A. Bigot, B. Jouffrey, P. Auger, S. Belliot, Ultramicroscopy 98 (2004) 219.
[26] S.J. Plimpton, J. Comput. Phys. 117 (1995) 1.
[27] F. Apostle, Y. Mishin, unpublished.
[28] M.S. Daw, M.I. Baskes, Phys. Rev. B 29 (1984) 6443.
[29] Y. Mishin, M. Mehl, D. Papaconstantopoulos, Acta Mater. 53 (2005) 4029.
[30] J. Li, Modell. Simul. Mater. Sci. Eng. 11 (2003) 173.
[31] C. Kelchner, S. Plimpton, J. Hamilton, Phys. Rev. B 58 (1998) 11085.